Chapter 5
Analysis of Sliding Mode Controllers in the Frequency Domain

Conventional sliding mode control, studied in Chap. 2, and second-order sliding mode control (Chap. 4) are the most obvious choices in controlling systems with bounded matched disturbances/uncertainties. Sliding mode control laws allow us achieve to insensitivity of system's compensated dynamics to these perturbations. The ultimate price for this insensitivity is a high-frequency (that is equal to infinity in an ideal sliding mode) switching control function that after being filtered by the plant yields self-sustained oscillations of almost zero amplitude. The main advantage of higher (second-)order sliding mode control is its ability to guarantee higher accuracy of the sliding variable stabilization at zero than conventional sliding mode control. Both conventional and second-order sliding mode control laws are derived (see Chaps. 2 and 4) assuming that the relative degree is equal to one in the case of conventional sliding mode control and equal to two for the case of second-order sliding modes. However, any real plant and any real switching element will contain parasitic dynamics that are not taken into account in the system's mathematical model. These parasitic dynamics increase the system's relative degree and could yield control chattering, i.e., self-sustaining oscillations of lower frequency and nonzero amplitude, causing degradation in the system's performance. In this chapter the robustness of the system in a sliding mode with respect to parasitic dynamics is studied using the *describing function technique*. This approximate technique is useful from a practical point of view for the analysis of self-sustained oscillation (limit cycles) as soon as the transient response is over.

5.1 Introduction

The phenomenon of chattering is caused by the inevitable existence of so-called *parasitic* or *unmodeled* dynamics that exist along with the *principal dynamics* of the plant. The *principal dynamics* are the dynamics of the plant model that are used for the SMC design. However, to implement the designed control algorithms, devices such as actuators and sensors are needed. These devices bring into the system certain

Y. Shtessel et al., *Sliding Mode Control and Observation*, Control Engineering,
DOI 10.1007/978-0-8176-4893-0_5,

parasitic dynamics that are not accounted for during the SMC design and which are treated as *unmodeled* dynamics at this step. Since the *parasitic* dynamics are usually connected in series with the *principal* dynamics, the combined relative degree of the actuator–plant–sensor becomes equal to the sum of the plant relative degree, the actuator relative degree, and the sensor relative degree.

It is known that conventional SMC in systems with parasitic dynamics of relative degree two or higher exhibit chattering.[1] For the same reason, it is logical to expect a similar behavior from systems with 2-SM controllers, as the above-mentioned 2-SM algorithms contain the sign function or infinite gains. In this chapter systems controlled by conventional SMC and all principal 2-SM controllers are analyzed in the frequency domain, while the parasitic/unmodeled dynamics are taken into account. The goal of this study is to analyze the robustness of the conventional SMC and the major 2-SM controllers, including the continuous super-twisting algorithm (see Chaps. 2 and 4), to parasitic/unmodeled dynamics by detecting possible self-sustained oscillations (limit cycles) and estimating their parameters (such as amplitude and frequency) via *describing function (DF) techniques* (see Appendix B). It is worth noting that the DF method provides only an approximate solution.[2]

5.2 Conventional SMC Algorithm: DF Analysis

Conventional SMC techniques rest on the concept of switching the system's structure in order to force the trajectory of the system to a switching surface and to maintain the system's motion on this surface thereafter. The system's motion on the sliding surface appeared to be insensitive to bounded model uncertainties and external disturbances (see Chap. 2). However, the robustness of conventional SMC to parasitic/unmodeled dynamics requires special consideration. It is expected that these dynamics may cause control chattering, which yields limit cycles and degradation in the system's performance. In many systems chattering is highly undesirable especially after the transient response is over. An analysis of self-sustained oscillations (limit cycles) in linear time-invariant systems with SMC and parasitic dynamics, via DF technique, is presented in this section. The linear system's principal dynamics are assumed to be given in Brunovsky's canonical form:

[1] This agrees with the classical research work on relay feedback systems theory [9, 181], where it was proven that for the plant of order 3 and higher the equilibrium point in the origin cannot be stable.

[2] There exists a method named the locus of a perturbed relay system Locus of Perturbed Relay System (LPRS) [29] that gives an exact analysis of limit cycles in perturbed relay systems. However, the LPRS method is computationally much more intensive than DF method. Conversely, the DF method is simple and efficient and provides accuracy sufficient for the analysis of practical systems.

$$\dot{x}(t) = A_p x(t) + B_p u(t) \tag{5.1}$$

where

$$A_p = \begin{bmatrix} 0 & 1 & 0 & \dots & 0 \\ 0 & 0 & 1 & \dots & 0 \\ .. & .. & .. & \dots & .. \\ -a_0 & -a_1 & -a_2 & \dots & -a_{n-1} \end{bmatrix} \qquad B_p = \begin{bmatrix} 0 \\ 0 \\ \vdots \\ b \end{bmatrix}$$

It is assumed that the characteristic polynomial

$$P(\lambda) = \lambda^n + a_{n-1}\lambda^{n-1} + \ldots + a_1\lambda + a_0$$

of system in (5.1) is Hurwitz.
The sliding variable is designed to have the form

$$\sigma = x_n + c_{n-1}x_{n-1} + \cdots + c_1 x_1 \tag{5.2}$$

The relative degree of the sliding variable in (5.2) is equal to one. Therefore, any conventional SMC that drives the sliding variable σ to zero in finite time can be designed by satisfying the sliding mode existence condition:

$$\sigma\dot{\sigma} \leq -\rho|\sigma| \tag{5.3}$$

The sliding mode control law is chosen as

$$u(t) = -U_m \text{sign}(\sigma) \tag{5.4}$$

where the modulation amplitude $U_m > 0$ is assumed to be chosen large enough.
The system's (5.1) dynamics in the sliding mode $\sigma = 0$ are derived:

$$\begin{cases} \dot{x}_1 = x_2 \\ \dot{x}_2 = x_3 \\ \dots \\ \dot{x}_{n-1} = -c_1 x_1 - c_2 x_2 - \cdots - c_{n-1}x_{n-1} \\ x_n = -c_1 x_1 - c_2 x_2 - \cdots - c_{n-1}x_{n-1} \end{cases} \tag{5.5}$$

In an ideal sliding mode, the frequency of switching of the control function (5.2) and (5.4) is infinite, while the sliding variable (5.2) oscillates with zero amplitude, and the state variables are continuous. However, parasitic dynamics may constrain the system's motion only to some vicinity of the switching surface $|\sigma| \leq \varepsilon > 0$ (a real sliding mode). In a real sliding mode, systems with SMC and parasitic dynamics can exhibit lower frequency self-sustained oscillation (chattering).

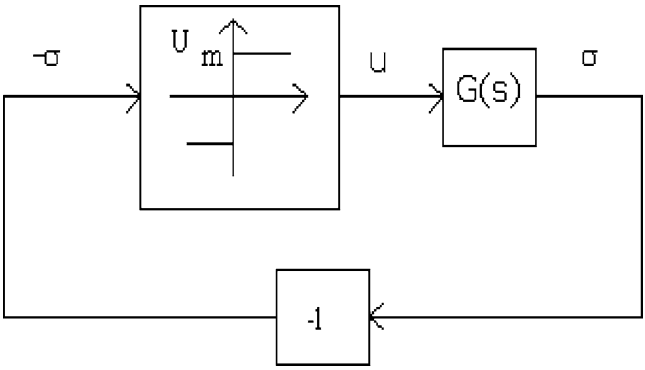

Fig. 5.1 Block diagram of a linear system with relay control and ideal sliding

Ideal Sliding Mode Analysis via DF Technique

The block diagram of the system (5.1), (5.2) and (5.4) is shown below in Fig. 5.1. The transfer function of the plant is identified as

$$G(s) = \frac{\sigma(s)}{u(s)} = \frac{b\left(s^{n-1} + c_{n-1}s^{n-2} + \ldots + c_2 s + c_1\right)}{s^n + a_{n-1}s^{n-1} + \ldots + a_1 s + a_0} \tag{5.6}$$

Assume that there exists a periodic motion (self-sustained oscillations or a limit cycle) with amplitude A_c and oscillation frequency ω_c in some vicinity of the switching surface (5.2) $|\sigma| \leq \varepsilon$ where $\varepsilon > 0$ in the system. In the frequency domain analysis we replace the Laplace variable s by $j\omega$, where ω is the frequency. Thus we assume that the following equation is valid:

$$-\sigma = A_c \sin(\omega_c) \tag{5.7}$$

The amplitude A_c and the oscillation frequency ω_c have to satisfy the harmonic balance equation (see Appendix B)

$$G(j\omega) = -\frac{1}{N(A,\omega)} \tag{5.8}$$

where the describing function of the relay nonlinearity is identified as follows:

$$N(A,\omega) = \frac{4U_m}{\pi A} \tag{5.9}$$

Definition 5.1. A strictly stable linear system[3] with a transfer function (5.6) will be strictly passive if and only if

[3]For details see [100].

$$|\arg G(j\omega)| < \frac{\pi}{2} \quad \forall \omega \in [0, \infty) \tag{5.10}$$

It is obvious that the phase characteristic of the transfer function (5.6) satisfies the following equality:

$$\lim [\arg G(j\omega)] = -\frac{\pi}{2} \quad as \quad \omega \to \infty \tag{5.11}$$
$$\lim [\arg G(j\omega)] = 0 \quad as \quad \omega \to 0$$

Assume that the coefficients $c_1, c_2, \ldots, c_{n-1}$ have been selected so that the passivity condition (5.10) is met. Then there exists a unique solution: the magnitude $A_c = 0$ and the frequency $\omega_c \to \infty$ of Eqs. (5.8) and (5.9). This fact is illustrated in the following example.

Example 5.1. Let the plant be given by the following equations:

$$\begin{aligned} \dot{x_1} &= x_2 \\ \dot{x_2} &= -x_1 - x_2 + u \\ \sigma &= x_1 + x_2 \end{aligned} \tag{5.12}$$

with control

$$u = -\text{sign}(\sigma) \tag{5.13}$$

In accordance with Fig. 5.1

$$G(s) = \frac{s+1}{s^2 + s + 1} \tag{5.14}$$

and the harmonic balance condition is given by two equations that equate the real and imaginary parts of Eq. (5.8):

$$\text{Re}\,[G(j\omega] = -\frac{\pi A}{4U_m} \tag{5.15}$$

i.e.,

$$\frac{1 - \omega + \omega^2}{(1-\omega^2)^2 + \omega^2} = -\frac{\pi A}{4U_m}$$

and

$$\frac{\omega^2}{(1-\omega^2)^2 + \omega^2} = 0 \tag{5.16}$$

The obvious solution of Eq. (5.15) and (5.16) is

$$A_c = 0, \ \omega_c \to \infty \tag{5.17}$$

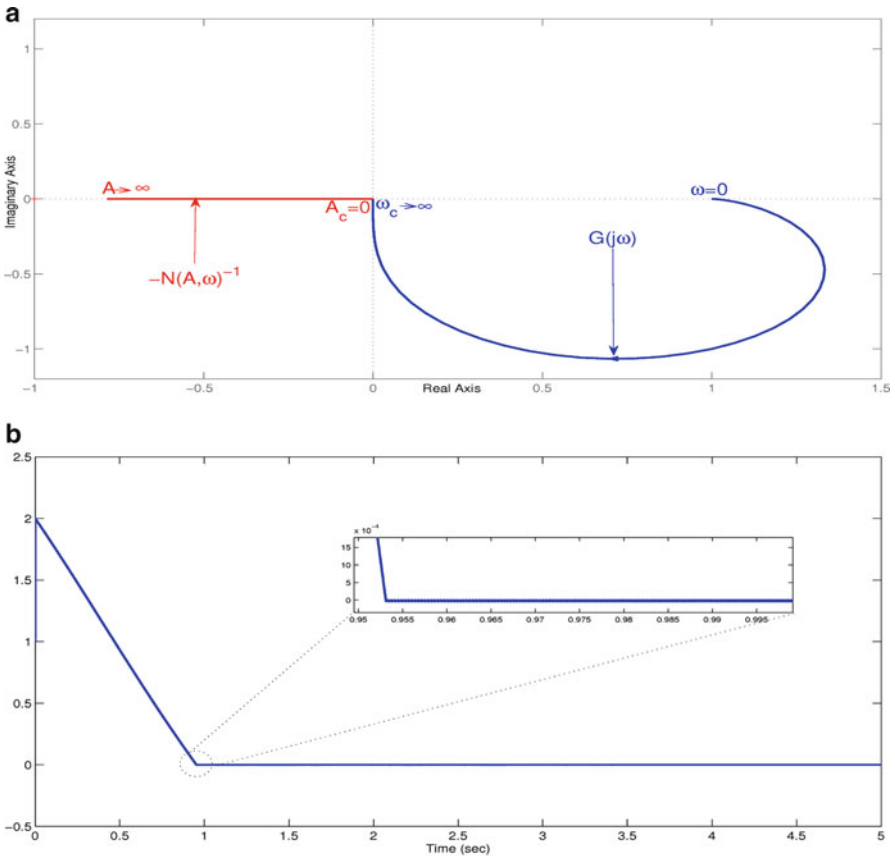

Fig. 5.2 Graphical solution of the harmonic balance equation for system $G(s)$. (**a**) Graphical solution. (**b**) Surface

This solution can be interpreted as a limit cycle with infinity frequency and zero amplitude that is expected in systems with ideal sliding mode control. The DF method does not give the opportunity to identify finite time or asymptotic convergence to the predicted limit cycle. A simple criterion for finite time convergence is achieved if the angle between the high-frequency asymptote of the Nyquist plot of the plant and the low-amplitude asymptote of the negative reciprocal of the describing function of the nonlinear element, the so-called *phase deficit*, is greater than zero. The graphical solution of the harmonic balance Eq. (5.8) that is presented in Fig. 5.2 confirms the solution given by (5.17) and also finite time convergence.

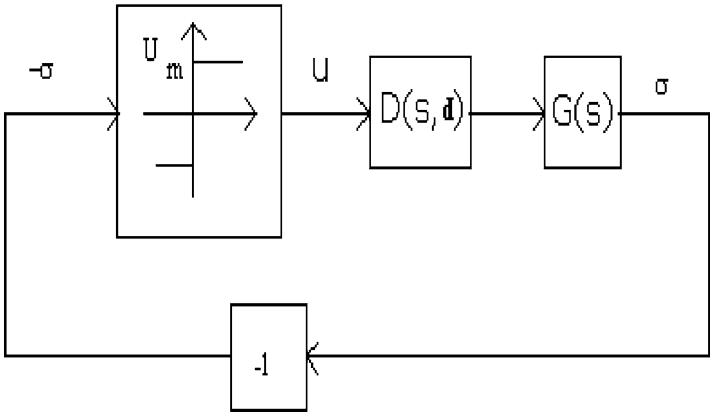

Fig. 5.3 Block diagram of linear system with relay control and parasitic dynamics

Real Sliding Mode Analysis via Describing Function Technique

Now system (5.1), (5.2) and (5.4) with parasitic dynamics is considered. The block diagram of this system is shown in Fig. 5.3 and the transfer function of the parasitic dynamics is

$$D(s,\mathbf{d}) = \frac{d_0}{s^k + d_{k-1}s^{k-1} + \ldots + d_1 s + d_0} \tag{5.18}$$

where the characteristic polynomial $P_d(\lambda) = \lambda^k + d_{k-1}\lambda^{k-1} + \ldots + d_1\lambda + d_0$ is Hurwitz.

In the system with parasitic dynamics given in (5.18) the relative degree of the sliding variable (5.2) is based on the combined principal (5.1) and parasitic dynamics (5.18) and is equal to $k+1$. Consequently, the sliding mode existence condition (5.3) cannot be met, which is why only a real sliding mode can exist in such a system.

Suppose the coefficients in the equation of the switching surface (5.2) are chosen such that the passivity condition (5.10) is met. It is obvious that the phase frequency characteristic of the transfer function $D(s,\mathbf{d})G(s)$ satisfies the following:

$$\lim\left[\arg D(j\omega,\mathbf{d})G(j\omega)\right] = -\frac{\pi}{2}(k+1) \quad as \quad \omega \to \infty \tag{5.19}$$

Therefore, the transfer function $D(s,\mathbf{d})G(s)$ is not passive for all $k \geq 1$. Assume that in the real sliding mode there exist self-sustained oscillations (limit cycle) with amplitude A_c and oscillation frequency ω_c in the system given by the block diagram

presented in Fig. 5.3. The amplitude A_c and the frequency of the oscillations ω_c can be computed based on the equation of harmonic balance:

$$D(j\omega, \mathbf{d})G(j\omega) = -\frac{1}{N(A,\omega)}, \quad N(A,\omega) = \frac{4U_m}{\pi A} \tag{5.20}$$

Assuming $k = 1$ it is obvious that there exists a unique solution: the magnitude $A_c = 0$ and the oscillation frequency $\omega_c \to \infty$. Real sliding mode control using the DF technique is illustrated in the next example.

Example 5.2. Let the plant with the actuator model be given by the following equations:

$$\begin{aligned} \dot{x_1} &= x_2 \\ \dot{x_2} &= -x_1 - x_2 + u \\ 0.01\dot{u_a} &= -u_a + u \\ \sigma &= x_1 + x_2 \end{aligned} \tag{5.21}$$

and the controller given by

$$u = -\text{sign}(\sigma) \tag{5.22}$$

In accordance with Fig. 5.3 we have

$$D(s,d)G(s) = \frac{s+1}{(0.01s+1)(s^2+s+1)} \tag{5.23}$$

The solution for the harmonic balance equation for the system associated with $D(s,d)G(s)$ is presented in Fig. 5.4.

Based on Fig. 5.4 we can conclude that the existence of an asymptotic limit cycle with $A_c = 0$ and $\omega_c \to \infty$ is predicted.

Assuming $k = 2$, it is obvious that there exists a unique solution with magnitude $A_c > 0$ and frequency $0 < \omega_c = C < \infty$ to Eq. (5.20). This fact is graphically illustrated in the following example.

Example 5.3. Let the plant with the actuator be given by the following equations:

$$\begin{aligned} \dot{x_1} &= x_2 \\ \dot{x_2} &= -x_1 - x_2 + u \\ 0.0001\ddot{u_a} &= -0.01\dot{u_a} - u_a + u \\ \sigma &= x_1 + x_2 \end{aligned} \tag{5.24}$$

The solution for the harmonic balance equation for system $D(s,\boldsymbol{d})G(s)$ is presented in Fig. 5.5a. Figure 5.5b shows a zoom of the intersection between $G(j\omega)$ and

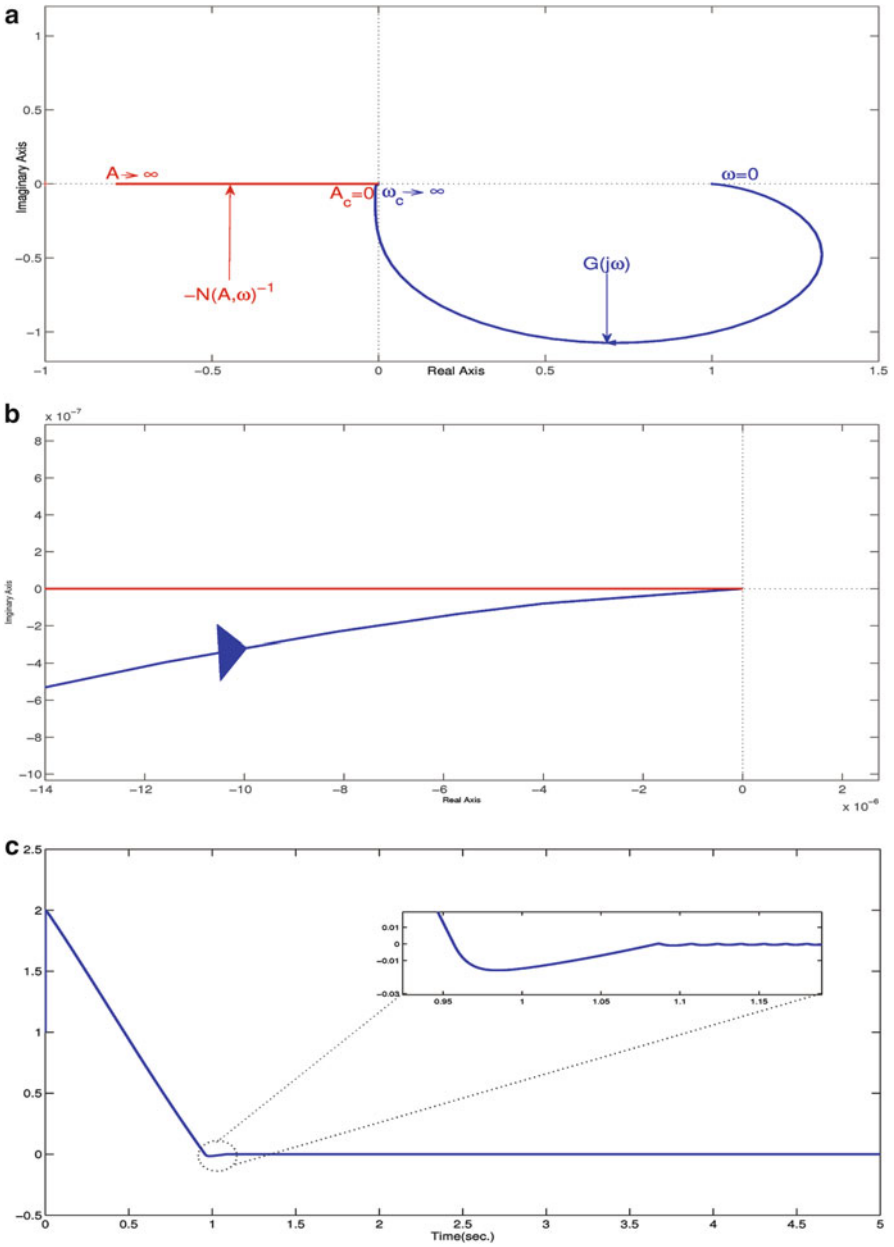

Fig. 5.4 Graphical solution of the harmonic balance equation for the system $D(s, \boldsymbol{d})G(s)$ with a first-order actuator. (**a**) Graphical solution. (**b**) Graphical solution zoom. (**c**) Surface

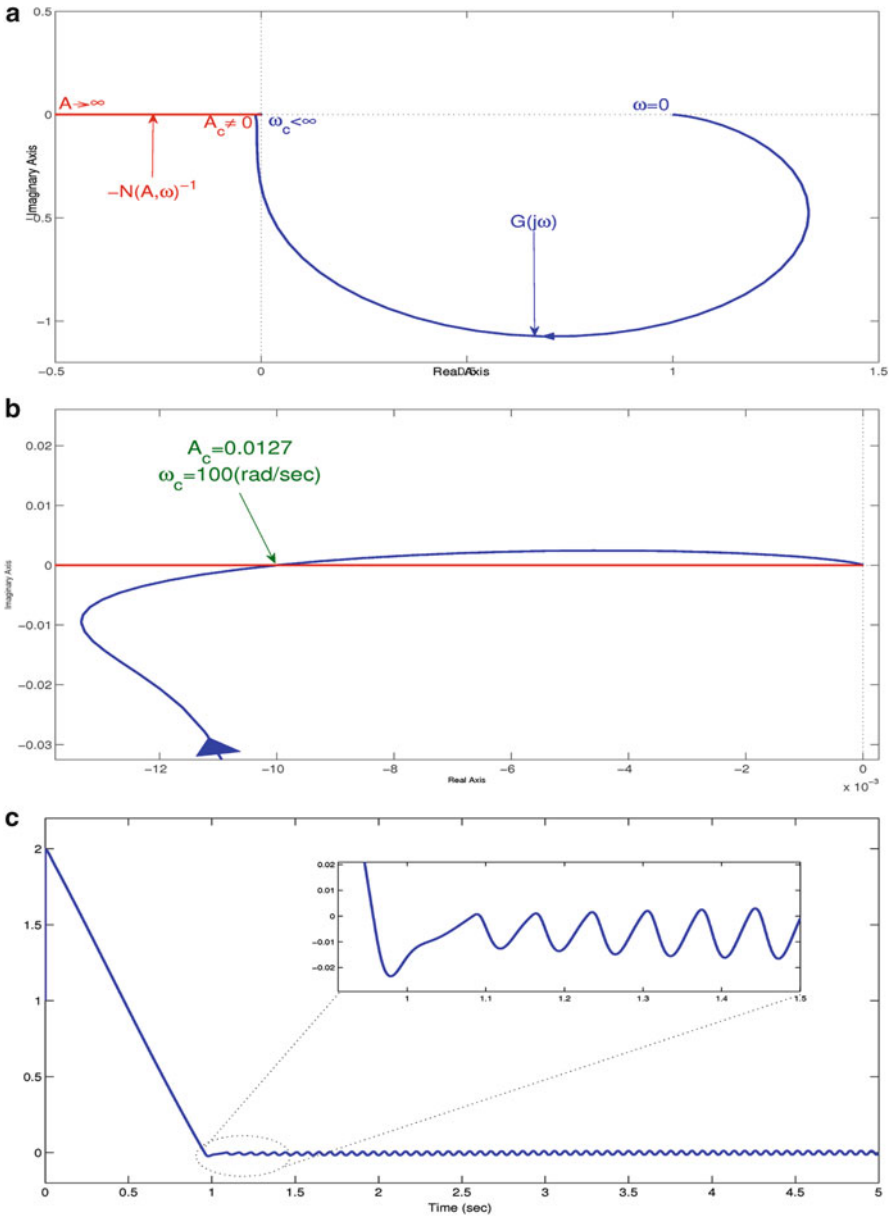

Fig. 5.5 Graphical solution of the harmonic balance equation for system $D(s,\boldsymbol{d})G(s)$ with second-order actuator. (**a**) Graphical solution. (**b**) Graphical solution zoom. (**c**) Surface

$N(A,\omega)^{-1}$ where we can see the value of the oscillation parameters. Based on Fig. 5.5b, c we can conclude the existence of a limit cycle with $A_c = 0.0127$ and $\omega_c = 100(rad/sec)$.

The results of the presented analysis are summarized in the following proposition:

Proposition 5.1. *If the switching surface (5.2) is designed to make the transfer function (5.6) strictly passive and the stable parasitic dynamics are given by Eq. (5.18), then in the system given by Eqs. (5.1), (5.2), (5.4) and (5.18) there exist:*

(a) An ideal sliding mode for $k = 0$
(b) An asymptotic sliding mode for $k = 1$
(c) A real sliding mode with chattering for $k \geq 2$

5.3 Twisting Algorithm: DF Analysis

The twisting algorithm (see Chap. 4) is one of the simplest and most popular algorithms among the second-order sliding mode algorithms. There are two ways of using the twisting algorithm: to apply it to the principal dynamics of a system of relative degree two or to apply it to the principal dynamics of a system of relative degree one and introduce an integrator in series with the plant (twisting as a filter). For the principal dynamics of relative degree two it can be formulated as follows. Let the plant (or the plant plus actuator) be given by the following differential equations:

$$\dot{x}(t) = Ax(t) + Bu(t), \quad \sigma = Cx \tag{5.25}$$

where A and B are matrices of appropriate dimensions, $x \in \mathbb{R}^n$, and $\sigma \in \mathbb{R}$ can be treated as either the sliding variable or the output of the plant. We assume that the plant is asymptotically stable, apart from some possible integrating terms, and is a low-pass filter. We shall also use the plant description in the form of a transfer function $W(s)$, which can be obtained from the formulas (5.25) as follows:

$$W(s) = C(Is - A)^{-1}B$$

Also, let the control u of the twisting algorithm be given as

$$u(t) = -\alpha_1 \text{sign}(\sigma) - \alpha_2 \text{sign}(\dot{\sigma}) \tag{5.26}$$

where α_1 and α_2 are positive values, $\alpha_1 > \alpha_2 > 0$.

Assume that a periodic motion occurs in the system with the twisting algorithm. The objective is to find the parameters of this periodic motion. The system will be analyzed with the use of the DF method. As normal in a DF analysis, we assume that the harmonic response of the plant is that of a low-pass filter, so that the output

of the plant is a harmonic oscillation. To find the DF of the twisting algorithm as the first harmonic of the periodic control signal divided by the amplitude of $\sigma(t)$,

$$N = \frac{\omega}{\pi A}\int_0^{2\pi/\omega} u(t)\sin(\omega t)dt + j\frac{\omega}{\pi A}\int_0^{2\pi/\omega} u(t)\cos(\omega t)dt \tag{5.27}$$

where A is the amplitude of the input to the nonlinearity (of $\sigma(t)$ in our case) and ω is the frequency of $\sigma(t)$. However, the twisting algorithm can be analyzed as the parallel connection of two ideal relays where the input to the first relay is the sliding variable and the input to the second relay is the derivative of the sliding variable. The DF for those nonlinearities are well known. For the first relay the DF is $N_1 = \frac{4\alpha_1}{\pi A}$ and for the second relay $N_2 = \frac{4\alpha_2}{\pi a_\sigma}$, where a_σ is the amplitude of $d\sigma/dt$. Also, we need to take into account the relationship between σ and $d\sigma/dt$ in the Laplace domain, which gives the relationship between the amplitudes A and a_σ as $a_\sigma = A\omega$, where ω is the frequency of the oscillation. Using the notation of the twisting algorithm we can write this as follows:

$$N = N_1 + sN_2 = \frac{4\alpha_1}{\pi A} + j\omega\frac{4\alpha_2}{\pi a_\sigma} = \frac{4}{\pi A}(\alpha_1 + j\alpha_2) \tag{5.28}$$

where $s = j\omega$. Note that the DF of the twisting algorithm depends on the amplitude value only. This suggests finding the parameters of the limit cycle via the solution of the harmonic balance equation:

$$W(j\omega)N(A) = -1 \tag{5.29}$$

where A is the generic amplitude of the oscillation at the input of the nonlinearity and $W(j\omega)$ is the complex frequency response characteristic (Nyquist plot) of the plant. Using the notation of the twisting algorithms this equation can be rewritten as follows:

$$W(j\omega) = -\frac{1}{N(A)} \tag{5.30}$$

where the function at the right-hand side is given by

$$-\frac{1}{N} = \pi A\frac{-\alpha_1 + j\alpha_2}{4(\alpha_1^2 + \alpha_2^2)}$$

Equation (5.29) is equivalent to the condition of the complex frequency response characteristic of the open-loop system intersecting the real axis at the point $(-1, j0)$. A graphical illustration of the technique of solving Eq. (5.29) is given in Fig. 5.6. The function $-\frac{1}{N}$ is a straight line whose slope depends on the ratio α_2/α_1. This line is located in the second quadrant of the complex plane. The point of intersection of this function and the Nyquist plot $W(j\omega)$ provides the solution of the periodic problem. This point gives the frequency of the oscillation ω_c and the amplitude A_c. Therefore, if the transfer function of the plant (or plant plus actuator) has relative

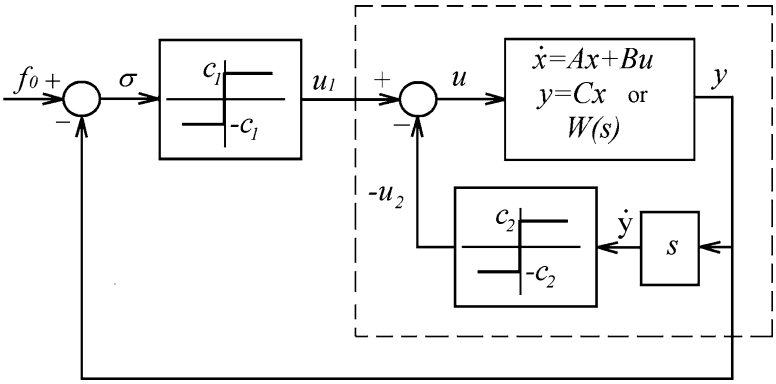

Fig. 5.6 Transformed system with twisting control

degree higher than *two* a periodic motion may occur in such a system. For that reason, if an actuator of first or higher order is added to the plant of relative degree *two* driven by the twisting controller, a periodic motion may occur in the system.

The conditions for the existence of a periodic solution in a system with the twisting controller can be derived from the analysis of Fig. 5.6. Obviously, every system with a plant of relative degree *three* and higher would have a point of intersection with the negative reciprocal of the DF of the twisting algorithm and, therefore, a periodic solution could exist.

Another modification of the twisting algorithm is its application to a plant with relative degree one with the introduction of an integrator (see Chap. 4). This is usually referred to as the "twisting as a filter" algorithm. The above reasoning is applicable in this case too. The introduction of the integrator in series with the plant makes the relative degree of this part of the system equal to two. As a result, any actuator introduced in the loop increases the overall relative degree to at least three. In this case, there always exists a point of intersection between the Nyquist plot of the serial connection of the actuator, the plant and the integrator, and of the negative reciprocal of the DF of the twisting algorithm (Fig. 5.7). Thus, if an actuator of first or higher order is added to the plant with relative degree one, a periodic motion may occur in the system with the "twisting as a filter algorithm.".

Remark 5.1. The asymptotic 2-SM relay controller

$$\ddot{x} = -a\dot{x} - bx - k\,\mathrm{sign}(x),\ a > 0, k > 0$$

can also be studied. It can be shown that this system is exponentially stable. With respect to our analysis, from Fig. 5.7, it also follows that the frequency of the periodic solution for the twisting algorithm is always higher than the frequency of the asymptotic second-order sliding mode relay controller, because the latter is determined by the point of intersection of the Nyquist plot and the real axis.

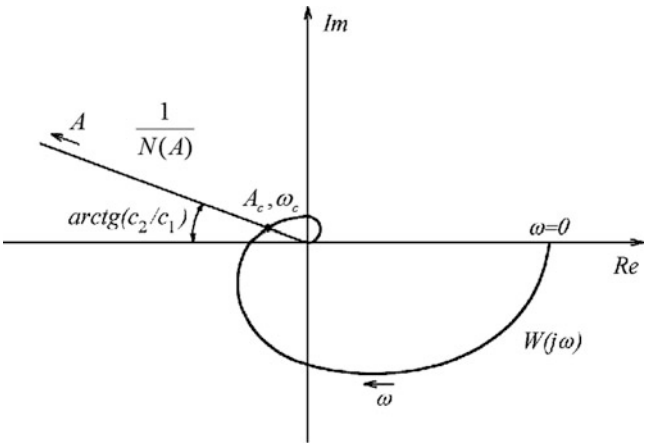

Fig. 5.7 Finding a periodic solution in system with twisting control

5.4 Super-Twisting Algorithm: DF Analysis

5.4.1 DF of Super-Twisting Algorithm

The super-twisting algorithm is probably one of the most popular second-order sliding mode algorithms. It is used for systems with principal dynamics of relative degree *one*. The control $u(t)$ for the super-twisting algorithm is given as a sum of two components:

$$u(t) = u_1(t) + u_2(t) \tag{5.31}$$

$$\dot{u}_1 = -\gamma \,\mathrm{sign}(\sigma)$$

$$u_2 = \begin{cases} -\lambda |s_0|^\rho \,\mathrm{sign}(\sigma), & \text{if} \quad |\sigma| > s_0 \\ -\lambda |\sigma|^\rho \,\mathrm{sign}(\sigma), & \text{if} \quad |\sigma| \le s_0 \end{cases}$$

where α, ρ, and s_0 are design parameters, with $0.5 \le \rho < 1$.

The system under analysis can be represented in the form of the block diagram as in Fig. 5.8.

For an arbitrary value of the power ρ in (5.31), the formula for the DF of such a nonlinear function can be given as follows:

$$N_2 = \frac{2\lambda A^{\rho-1}}{\pi} \int_0^\pi (\sin(\psi))^{\rho+1} d\psi = \frac{2\lambda A^{\rho-1}}{\sqrt{\pi}} \frac{\Gamma(\frac{\rho}{2}+1)}{\Gamma(\frac{\rho}{2}+1.5)} \tag{5.32}$$

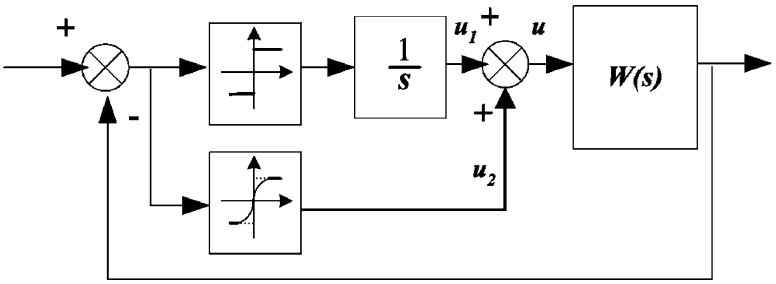

Fig. 5.8 Block diagram of a linear system with super-twisting control

where $0 < \rho < 1$, A is the amplitude of the variable y, $A \leq s_0$ (this is considered as the most important range of the amplitude values for the analysis of the steady state), and Γ is the gamma function.[4]

With the square root nonlinearity ($\rho = 0.5$) the DF formula can be derived as

$$N_2 = \frac{2\lambda}{\pi A}\int_0^{\pi} \sqrt{A\sin(\psi)}\sin(\psi)d\psi = \frac{2\lambda}{\sqrt{\pi A}}\frac{\Gamma(1.25)}{\Gamma(1.75)} \approx \frac{1.1128\lambda}{\sqrt{A}} \tag{5.33}$$

The DF of the first component of the super-twisting algorithm can be written:

$$N_1 = \frac{4\gamma}{\pi A}\frac{1}{j\omega}$$

which is a result of the cascade connection of the ideal relay having a DF equal to $\frac{4\gamma}{\pi A}$ and an integrator with transfer function $1/s$ (for the harmonic signal, the Laplace variable s can be replaced with $j\omega$). Taking into account both control components, we can rewrite the DF of the super-twisting algorithms as

$$N = N_1 + N_2 = \frac{4\gamma}{\pi A}\frac{1}{j\omega} + \frac{1.1128\lambda}{\sqrt{A}} \tag{5.34}$$

Note that the DF of the super-twisting algorithm depends on both the amplitude and the frequency values. The parameters of the limit cycle can be found via the solution of the harmonic balance Eq. (5.29), where the DF N is given by (5.34). The negative reciprocal of the DF can be represented by the following formula:

$$-\frac{1}{N} = \frac{1}{1.1128\frac{\lambda}{\sqrt{A}} + \frac{4\gamma}{\pi A}\frac{1}{j\omega}} = -\frac{0.8986\frac{\sqrt{A}}{\lambda} + j1.1329\frac{\gamma}{\lambda^2}\frac{1}{\omega}}{1 + 1.3092\frac{\gamma^2}{\lambda^2}\frac{1}{A\omega^2}}$$

[4]For details, see, for example,[39].

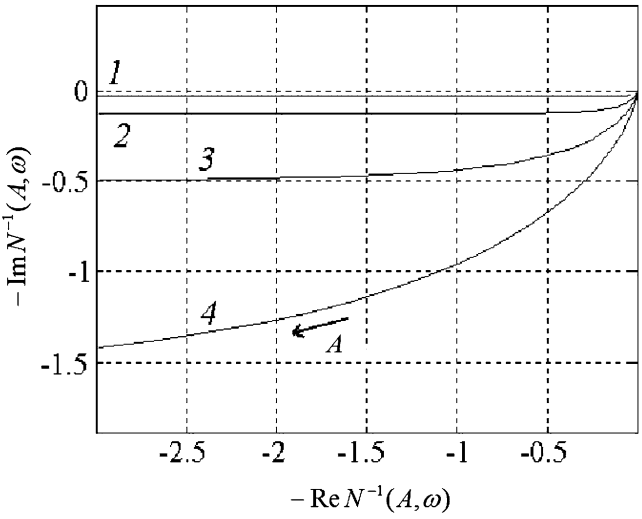

Fig. 5.9 Plots of the function $-1/N$ for super-twisting control

Now $-1/N$ is a function of two variables: the amplitude and the frequency. It can be depicted as a number of plots representing the amplitude dependence, with each of those plots corresponding to a certain frequency. The frequency range of interest lies below the frequency corresponding to the intersection of the Nyquist plot and the real axis. The plots of the function $-1/N$ are depicted in Fig. 5.9. Plots 1–4 correspond to four different frequencies, with the following relationship: $\omega_1 > \omega_2 > \omega_3 > \omega_4$. Each of these plots represents the dependence of the DF on the amplitude value.

The function $-N^{-1}(A)$ (where ω=const) has an asymptote as $A \to \infty$, which is the horizontal line $-j1.1329\frac{\gamma}{\lambda^2}\frac{1}{\omega}$. Also, it is easy to show that

$$\lim_{A\to 0} \arg(-N^{-1}(A), \omega) = -\pi/2$$

5.4.2 *Existence of the Periodic Solutions*

The solution of the harmonic balance Eq. (5.29) can be computed numerically by the application of various iterative techniques. However, the complex Eq. (5.29) with two unknown variables, A and ω, can be reduced to one real equation having only one unknown variable ω as follows. Write Eq. (5.29) in the form of $N(A) = -W^{-1}(j\omega)$, where $N(A)$ is given by (5.34):

$$\frac{4\gamma}{\pi A}\frac{1}{j\omega} + 1.1128\frac{\lambda}{\sqrt{A}} = -W^{-1}(j\omega) \tag{5.35}$$

Considering the real part of both sides we can obtain

$$1.1128\frac{\lambda}{\sqrt{A}} = -\operatorname{Re} W^{-1}(j\omega) \tag{5.36}$$

Eliminating A from the Eqs. (5.35) and (5.36) an equation with one unknown variable ω can be obtained as follows:

$$\Psi(\omega) = \frac{4\gamma}{\pi\omega}\frac{1}{\operatorname{Im} W^{-1}(j\omega)} - \left(\frac{1.1128\lambda}{\operatorname{Re} W^{-1}(j\omega)}\right)^2 = 0 \tag{5.37}$$

Once Eq. (5.37) has been solved, the amplitude of oscillation A_c can be computed as follows:

$$A_c = \frac{4\gamma}{\pi\omega_c}\frac{1}{\operatorname{Im} W^{-1}(j\omega_c)} \tag{5.38}$$

where ω_c is the frequency of the oscillations.

Therefore, if a periodic motion occurs, its parameters can be estimated from (5.37) and (5.38).

Proposition 5.2. *If the relative degree of the plant is two or higher and the plant does not have double zero poles, then at least one periodic solution of the system with the super-twisting algorithm can be always predicted and estimated using the DF technique.*

Proof. We first prove Proposition 5.2 for plants of relative degree three and higher. It follows from the formula of the DF of the algorithm (5.34) that a periodic solution should always be looked for within the frequency range that corresponds to $-\pi/2$ and $-\pi$ of the phase characteristic of the plant (see also Fig. 5.9). Denote by ω_1 the frequency where the phase characteristic of the plant is $-\pi/2$ (assuming that there is only one such frequency). Similarly denote the frequency ω_2 as the frequency at which the phase characteristic of the plant is $\arg W(j\omega_2) = -\pi$. Both frequencies are finite. Find the following two limits of the function from (5.37): $\Psi(\omega_1+) = -\infty$ and $\Psi(\omega_2-) = \infty$. Now observe that the signs are different and that the function $\Psi(\omega)$ is continuous within the range $\omega \in (\omega_1, \omega_2)$ [This follows from (5.37).] Therefore, within the specified range, there exists at least one solution of Eqs. (5.25) and (5.31). Assume now that the relative degree of the plant is two. In this case, we can define the frequency ω_1 in the same manner as before, but the frequency ω_2 becomes infinite. Write the asymptotic representation of the plant transfer function for high-frequency inputs in a polynomial form:

$$W(s) \approx \frac{1}{a_2 s^2 + a_1 s + a_0}$$

Then, substituting $j\omega$ for s, we obtain $W^{-1}(j\omega) \approx -a_2\omega^2 + a_0 + ja_1\omega$, and it is easy to see that for sufficiently large ω,

$$\Psi(\omega) = \frac{4\gamma}{\pi}\frac{1}{a_1\omega^2} - \frac{1.1128^2\lambda^2}{(a_0 - a_2\omega^2)^2} > 0$$

Therefore, between ω_1 and ω_2, there always exists a certain frequency ω, which provides a solution to Eq. (5.37). This completes the proof. □

Remark 5.2. It is important that the point of intersection is located in the third quadrant of the complex plane. Therefore, if the transfer function of the plant (or the plant plus actuator) has relative degree higher than one, a periodic motion may occur in such a system. For that reason, if *parasitic dynamics* of first or higher order are added to the *principal dynamics of* a relative degree one system driven by the super-twisting controller, a periodic motion may occur in the system. From Fig. 5.9, it also follows that the frequency of the periodic solution for the super-twisting algorithm is always lower than the frequency of the periodic motion in the system with the conventional first-order SM relay controller, because the latter is determined by the point of the intersection of the Nyquist plot and the real axis.

5.4.3 Stability of Periodic Solution

Proposition 5.3. *If the following inequality holds then the periodic solution given by Eq. (5.37) is locally stable:*

$$\mathrm{Re}\,\frac{h_1(A,\omega)}{h_2(A,\omega) + N(A,\omega)\frac{\partial \ln W(s)}{\partial s}\,|_{s=j\omega}} < 0 \tag{5.39}$$

where $h_1(A,\omega) = \frac{1.1128\lambda}{2A^{\frac{3}{2}}} - j\frac{4\gamma}{\pi\omega A^2}$, $h_2(A,\omega) = \frac{4\gamma}{\pi\omega^2 A}$.

Proof. To investigate the local stability of the solution of (5.37), we consider the system transients due to small perturbations of this solution when A is quasi-statically varied to $(A + \triangle A)$. Here we assume that the harmonic balance equation still holds for small perturbations, so that a damped oscillation of the complex frequency $j\omega + (\triangle\sigma + j\Delta\omega)$ corresponds to the modified amplitude $(A + \triangle A)$:

$$N(A + \triangle A, j\omega + (\triangle\sigma + j\Delta\omega))W(j\omega + (\triangle\sigma + j\Delta\omega)) = -1 \tag{5.40}$$

where the DF $N(A,\omega)$ is given by Eq. (5.34). The nominal solution is determined by zero perturbations: $\triangle\sigma = \Delta\omega = \triangle A = 0$. By considering variations around the nominal solution defined by ω and A, let us find the conditions when $\Lambda = \triangle\sigma/\triangle A$ is negative. First write an equation for the amplitude perturbation $\triangle A$. For that purpose take the derivative of (5.40) with respect to $\triangle A$ as follows:

$$\left\{ \frac{dN(\triangle A, \triangle\sigma, \Delta\omega)}{d\triangle A}|_{\triangle A=0} W(j\omega) + \frac{dW(\triangle\sigma, \Delta\omega)}{d\triangle A}|_{\triangle A=0} N(A,\omega) \right\} \triangle A = 0 \tag{5.41}$$

Taking derivatives of N and W, and considering their composite functions, we obtain

$$\frac{dN(\triangle A, \triangle\sigma, \Delta\omega)}{d\triangle A}|_{\triangle A=0} = -j\frac{4\gamma\omega}{\pi A^2} - \frac{1.1128\lambda}{2A^{\frac{3}{2}}} + \frac{4\gamma A}{\pi\omega^2}\left(\frac{d\triangle\sigma}{d\triangle A} + j\frac{d\triangle\omega}{d\triangle A}\right) \tag{5.42}$$

$$\frac{dW}{d\triangle A}|_{\triangle A=0} = \frac{dW}{ds}|_{s=j\omega}\left(\frac{d\triangle\sigma}{d\triangle A} + j\frac{d\triangle\omega}{d\triangle A}\right) \tag{5.43}$$

Solving (5.41) for $(\frac{d\triangle\sigma}{d\triangle A} + j\frac{d\triangle\omega}{d\triangle A})$ and taking account of (5.42) and (5.44), we can obtain an analytical formula. Considering only the real part of this formula we obtain (5.39). This completes the proof. □

5.5 Prescribed Convergence Control Law: DF Analysis

The prescribed convergence control law is given as follows:

$$u = -\lambda \text{sign}(\dot{\sigma} + \beta|\sigma|^{\rho}\,\text{sign}(\sigma))$$

with $0.5 < \rho < 1$. The system under analysis can be represented in the form of the block diagram as in Fig. 5.10. In an autonomous mode (i.e., with no input signal), the error signal is equal to the negative output. Assuming that a periodic motion occurs, the objective is to find the parameters of this periodic motion. The controller has one input and, for that reason, a describing function of the algorithm can be obtained in accordance with the definition given in (5.27) above. As previously, assume that $\sigma(t) = Asin(\omega t)$. Applying Eq. (5.27) to the nonlinear

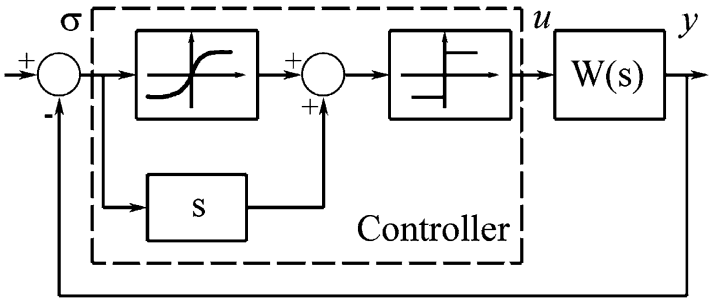

Fig. 5.10 Block diagram of a linear system with prescribed convergence control law

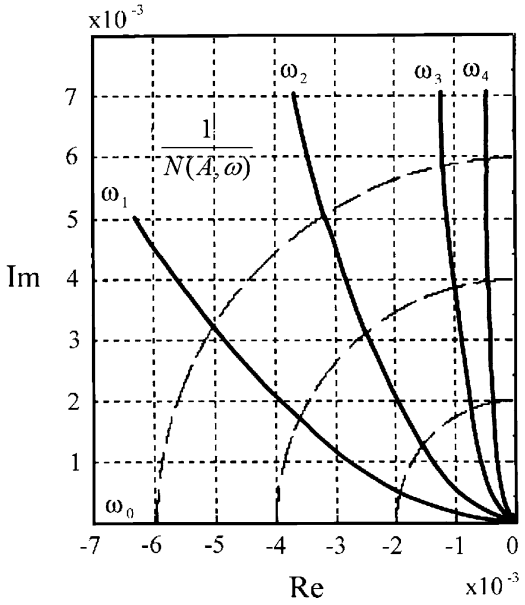

Fig. 5.11 Plots of the function $-1/N$ for the prescribed control law

function denoted as a dashed rectangle in Fig. 5.10, the describing function of the algorithm can be easily obtained. For the prescribed control law, the DF is a function of not only the amplitude but also of the frequency. The DF can be found only algorithmically. The values of the negative reciprocal of the DF are given in Fig. 5.11 as functions of the amplitude A for a few discrete values of the frequency $\omega(0 < \omega_1 < \omega_2 < \omega_3 < \omega_4, \omega_0 = 0)$. The function $-N_1^{-1}(A, \omega)$ (where $\omega =$const) is completely located in the second quadrant. Two limiting cases for the frequencies $\omega \to 0$ and $\omega \to \infty$ correspond to the real half axis and to the imaginary half axis, respectively. Note that the magnitude of the describing function for the prescribed control law does not depend on frequency and is given by the following formula: $|N| = 4\lambda/(\pi A)$. In Fig. 5.11, the contours representing equal values of A are depicted as dash lines. The Nyquist plot of any plant of relative degree *three* or higher will have a point of the intersection with the plot $N_1^{-1}(A, \omega)$ because the former is located in the second quadrant of the complex plane. Therefore, if the transfer function of the plant has relative degree higher than *two*, a periodic motion may occur in such a system. For that reason, if an actuator of first or higher order is added to the plant with relative degree two driven by the prescribed control law, a periodic motion may occur. From Fig. 5.11, it also follows that the frequency of the periodic solution for the prescribed control law algorithm is always higher than the frequency of the periodic motion in the system with the asymptotic 2-SM relay controller, because the latter is determined by the point of the intersection of the Nyquist plot and the real axis.

5.6 Suboptimal Algorithm: DF Analysis

Now consider the generalized suboptimal algorithm given as follows:

$$u(t) = -\alpha(t)U_M \text{sign}(\sigma(t) - \beta\sigma_M(t)) \tag{5.44}$$

$$\alpha(t) = \begin{cases} 1 & \text{if} \quad \sigma_M(t)(y(t) - \beta\sigma_M(t)) \geq 0 \\ \alpha^*, & \text{if} \quad \sigma_M(t)(y(t) - \beta\sigma_M(t)) < 0 \end{cases}$$

where $\sigma_M(t)$ is a piecewise constant function representing the value of the last singular point of $\sigma(t)$ (i.e., the most recent value of $\sigma(t)$ satisfying the condition $\dot{\sigma}(t) = 0$), U_M is the control amplitude, $\beta \in [0, 1)$ is the anticipation parameter, and $\alpha^* \geq 1$ is the modulation parameter. Let us assume that the steady-state behavior of the system (5.25) and (5.44) is a periodic, unimodal symmetric motion with zero mean and shows that the motion under this assumption can exist. The sequence of singular points of the variable $\sigma(t)$ is then an alternating sequence of positive and negative values of the same magnitude: σ_M^P, $-\sigma_M^P$, $\beta\sigma_M^P$, $-\beta\sigma_M^P$ (where "P" stands for periodic). The switching of the control occurs at the instants when the plant output $\sigma(t)$ becomes equal either to σ_M^P or to $\beta\sigma_M^P$. This would correspond to the following nonlinear characteristic of the controller (Fig. 5.12).

With this representation, the DF method can be conveniently used for analysis of the system with the suboptimal algorithm. The usual assumption for applicability of the DF method is the linear part (the combined *principal* and *parasitic* dynamics)

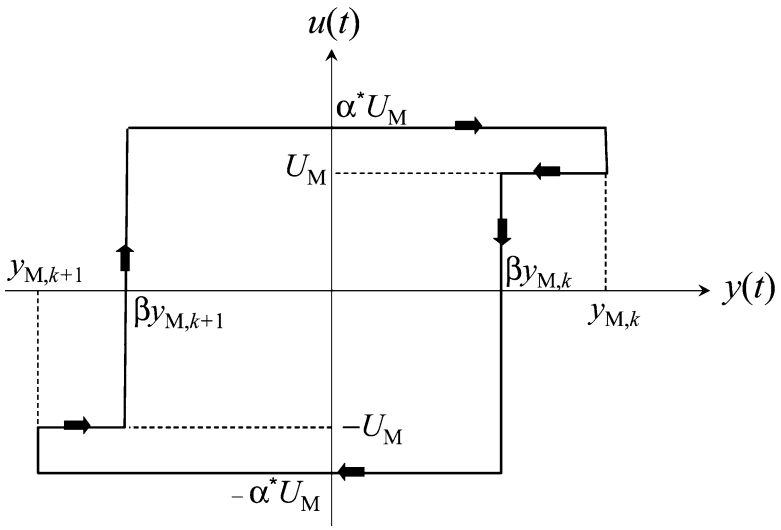

Fig. 5.12 Nonlinear characteristic of sub-optimal control

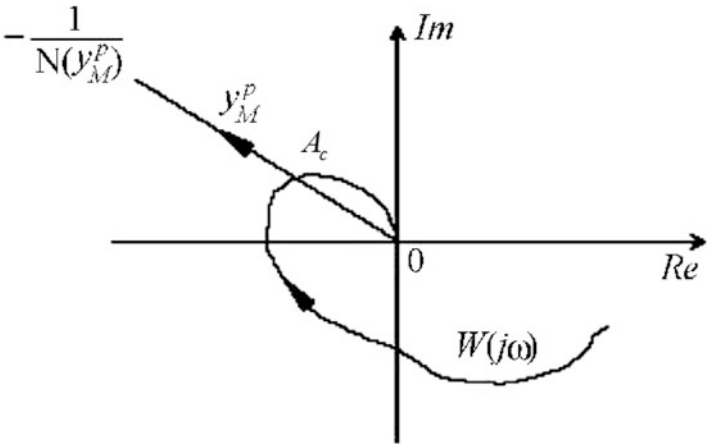

Fig. 5.13 Finding a periodic solution in a system with suboptimal control

satisfying the filtering hypothesis. As a result, the DF of the suboptimal algorithm can be given by the following equation:

$$N(A) = \frac{2U_M}{\pi A}\left\{(\alpha^* + 1)\sqrt{1-\beta^2} + j\left[(\alpha^* - 1) + \beta(\alpha^* + 1)\right]\right\} \tag{5.45}$$

where $A = \sigma_M^P$ is the amplitude of the oscillations of the output. A periodic solution of the system (5.25) and (5.44) takes place if the negative reciprocal of the DF has a point of intersection with the Nyquist plot of the linear part of the system. The negative reciprocal of the DF (that corresponds to the amplitude) is

$$-\frac{1}{N(A)} = -\frac{\pi A}{4U_M}\left\{\frac{(\alpha^* + 1)\sqrt{1-\beta^2}}{\alpha^{*2}(\beta+1) + (1-\beta)} + j\frac{(\alpha^* - 1) + \beta(\alpha^* + 1)}{\alpha^{*2}(\beta+1) + (1-\beta)}\right\} \tag{5.46}$$

The negative reciprocal of the DF is a straight line in the complex plane that begins at the origin ($A = 0$) and makes a clockwise angle with the negative part of the real axis. The plot is totally located in the second quadrant (Fig. 5.13).
From (5.46), the angle ϕ between the real axis and the line can be obtained as follows:

$$\phi = -\arctan\frac{(\alpha^* - 1) + \beta(\alpha^* + 1)}{(\alpha^* + 1)\sqrt{1-\beta^2}} \tag{5.47}$$

The frequency of possible periodic motions is the frequency of the Nyquist plot of the plant at the point of intersection with the plot $-\frac{1}{N(A)}$. This can be expressed as the solution of the following nonlinear equation:

$$\arg W(j\omega) = -\pi - \phi \tag{5.48}$$

where ϕ is given by Eq. (5.47), ω is the frequency of the periodic solution, and $W(s)$ is the transfer function of the combined *parasitic* and *principal* dynamics.

The amplitude of this periodic motion depends on the magnitude of the frequency response $W(j\omega)$ of the plant at the frequency ω. Usually a larger value of ϕ provides a higher frequency and a smaller amplitude of the periodic motion. The amplitude A_c of the periodic motion can be evaluated as follows:

$$A_c = \frac{2\sqrt{2}U_m\sqrt{\alpha^{*2}(1+\beta)+1-\beta}}{\pi}|\arg W(j\omega_c)| \tag{5.49}$$

where ω_c is the frequency of the oscillations.

It follows from (5.47) that the range of ϕ values is $[0; \pi/2]$. Therefore, a periodic motion may occur if the phase characteristic of the combined *parasitic* and *principal* dynamics includes the range from $-\pi$ to -1.5π. This is only possible if the combined relative degree of the *parasitic* and *principal* dynamics is three or higher (however, there may be some cases when the phase characteristic a plant of relative degree lower than three can go below $-\pi$).

5.7 Comparisons of 2-Sliding Mode Control Algorithms

The examples which have been studied confirm the properties of the algorithms and also demonstrate high accuracy—the DF analysis matches very accurately the results of the simulations (see Tables 5.1–5.4). In the simulations the following values of control algorithm parameters have been used: for the twisting algorithm

Table 5.1 Results of computing and simulations for the system with the plant of relative degree two $W_p(s) = \frac{1}{s^2+s+1}$ and an actuator of relative degree one $W_a(s) = \frac{1}{0.01s+1}$ driven by the 2-SM control algorithms

	Twisting	Prescribed	Suboptimal
ω_c (DF analysis)	77.05	80.85	59.81
ω_c (simulations)	77.68	81.72	55.16
Amplitudes, A_c	1.67e-4	1.51e-4	3.6e-4

Table 5.2 Results of computing and simulations for the system with the plant of relative degree two $W_p(s) = \frac{1}{s^2+s+1}$ and an actuator of relative degree two $W_a(s) = \frac{1}{0.0001s^2+0.01s+1}$ driven by the 2-SM control algorithms

	Twisting	Prescribed	Suboptimal
ω_c (DF analysis)	54.64	63.10	50.83
ω_c (simulations)	54.53	61.60	50.67
Amplitudes, A_c	4.83e-4	3.67e-4	4.63e-4

Table 5.3 Results of computing and simulations for the system with the plant of relative degree one $W_p(s) = \frac{s+1}{s^2+s+1}$ and an actuator of relative degree one $W_a(s) = \frac{1}{0.01s+1}$ driven by the 2-SM control algorithms

	Twisting as a filter	Super-twisting	Conventional SMC
ω (DF analysis)	75.00	66.16	∞
ω (simulations)	75.51	64.96	Converge to ∞
Amplitudes, A_c	2.53e-6	2.33e-4	0

Table 5.4 Results of computing and simulations for the system with the plant of relative degree one $W_p(s) = \frac{s+1}{s^2+s+1}$ and an actuator of relative degree two $W_a(s) = \frac{1}{0.0001s^2+0.01s+1}$ driven by the 2-SM control algorithms

	Twisting as a filter	Super-twisting	Conventional SMC
ω (DF analysis)	53.52	55.18	100.00
ω (simulations)	53.41	54.26	99.26
Amplitudes, A_c	9.48e-6	4.81e-4	1.27e-4

$c_1 = 0.8, c_2 = .0.6$; for the prescribed control law $\lambda = \beta = 1, \rho = 0.5$; for the sub optimal algorithm $\alpha^* = 1, \beta = 0.5$; and for the super-twisting algorithm $\lambda = 0.6, \gamma = 0.8, \rho = 0.5$.

The presented analysis demonstrates that the 2-SM control *algorithms cannot be chattering-free although the algorithms are continuous*. A frequency domain analysis of the known 2-SM control algorithms proves that very convincingly. Furthermore the cause of chattering is the inevitable existence of *parasitic* (not accounted for in the 2-SM controller design) dynamics associated with the actuators, sensors, etc.

However, new algorithms may be developed in the future that may be claimed to be chattering-free. Of course, an individual frequency-domain analysis of each available algorithm can provide some clues, but a more detailed analysis of the principles the 2-SM is based on would be very useful and might prevent wishful but wrong conclusions in the future.

The frequency-domain analysis which has been presented leads to the formulation of *two* ideas or *two* frequency-domain interpretations of the 2-SM controller designs. Those ideas are (1) an *advance switching* and (2) *control smoothing* due to introduction of an integrator. The first principle is applied to plants of relative degree two, and the second principle is applied to the plants of relative degree *one*. Let us consider those two principles in more detail.

The *advance switching* idea is used in the twisting algorithm, prescribed control law, and suboptimal algorithm. The advance switching is different in comparison with the switching in the conventional relay feedback control and is achieved by introducing phase-lead elements (differentiators) into the system loop or from the use of the negative hysteresis of the relay nonlinearity. In the frequency domain it is manifested as the location of the negative reciprocal of the DF of the respective algorithm in the second quadrant of the complex plane (see Figs. 5.6, 5.11, and 5.13).

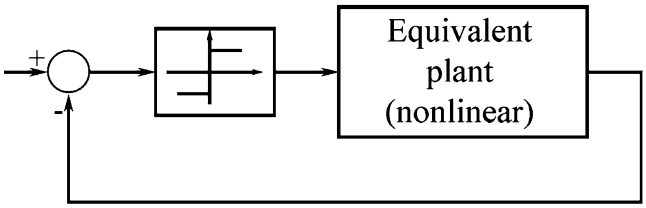

Fig. 5.14 Equivalent relay system

The *control smoothing* idea is realized via introducing an integrator in series with one of the 2-SM control algorithms which have advance switching or a relay nonlinearity (the super-twisting algorithm). This idea essentially exploits the stability margins of a relay control system with a plant of relative degree *one*, since the addition of one more relative degree does not cause finite frequency periodic motions in such systems. However, the introduction of the integrator in series with the *principal dynamics* of relative degree *one* makes the relative degree of this part of the system equal to *two*. As a result, any *parasitic dynamics* increases the overall relative degree to at least *three*. In this case, there always exists a point of intersection between the Nyquist plot of the serial connection of the actuator, the plant and the integrator, and the negative reciprocal of the DF of the SMC algorithm. Thus, if *parasitic dynamics* of relative degree *one* or higher are added to the *principal dynamics* of relative degree *one*, a periodic motion may occur in the system. Therefore, the existence of parasitic dynamics makes the existence of chattering unavoidable even in the case of the continuous control algorithms.

From the above analysis, the following observation can be formulated: regardless of the algorithm, if the system relative degree (that includes the actuator, plant, and the algorithm itself if the latter contains integrators) is three or higher, a periodic motion may occur in the system. Let us analyze this fact on the basis of the DF method. First note that any 2-SM control algorithm contains the relay (sign) function. After that let us transform the original system into the conventional relay feedback system notation. In Fig. 5.14, the equivalent plant, which now includes the original plant, actuator, and all parts of the 2-SM control algorithm except for the relay element, is nonlinear. However, the nonlinearities of this equivalent plant do not change the order and relative degree of the equivalent plant. Consequently they can be replaced with some gains (which is what was done in the DF analysis above). Therefore, a property which is known for the relay systems should also apply to the equivalent relay system in Fig. 5.14. It can be formulated as the possibility of the existence of a periodic motion if the relative degree is *three or higher* and the existence of an ideal sliding mode otherwise.

The nature of the parasitic dynamics is the dynamics of energy transformation from one form to another. For example, an actuator is supposed to transform an electrical signal into a force or mechanical motion, and a sensor has to transform mechanical motion into an equivalent electrical signal. It follows from first principles that the relative degree of the actuator–plant–sensor dynamics will always

be higher than two. Moreover, even lower levels of detail can be considered, if necessary, such as delays in the electronics, resistance, capacitance, and inductance of the wires. If we assume that an ideal sliding mode exists in the system in Fig. 5.14, this is equivalent to assuming that the SMC generates a discontinuous control of infinite frequency, which cannot occur in any real system. For that reason, any implementation of the 2-SM control system (as well as a conventional SMC system) will always exhibit chattering. Thus, if for some sliding mode design, we obtained results corresponding to an ideal sliding mode that only means that the parasitic dynamics were either not considered or not considered in sufficient detail. Chattering is an inherent property of the sliding mode principal. The problem is therefore in controlling the parameters of the chattering and adjusting them to acceptable values. The approach presented here can be of significant help in achieving those goals.

5.8 Notes and References

DF analysis can give (predict) only the approximate limit cycle solution. The early results on the analysis of self-sustained oscillations in systems with conventional SMC can be found in [161]. A precise limit cycle analysis can be undertaken in 2-sliding systems using the LPRS technique presented in [29].

It is worth noting that the nonlinearity in Fig. 5.12 can be represented as a sum of two conventional hysteresis relays, for which the DFs are known [11].

The criterion for finite time convergence in terms of the angle between the high-frequency asymptote of the Nyquist plot of the plant and the low-amplitude asymptote of the negative reciprocal is given in [30].

A detailed analysis of self-sustained oscillations (chattering) in 2-SM systems is given in [28–30, 32, 34, 35, 88–90, 117, 150]. The analysis of the propagation of periodic signals for the systems governed by 2-SM control is studied in [36]. The self sustained oscillations in mechanical systems are studied in [4, 5].

5.9 Exercises

Exercise 5.1. Study a real sliding mode in the system

$$\begin{aligned} \dot{x_1} &= x_2 \\ \dot{x_2} &= -2x_1 - 3x_2 + u_a \\ 0.0001\ddot{u_a} &= -0.01\dot{u_a} - u_a + u \\ \sigma &= x_1 + x_2 \end{aligned}$$

with the controller

$$u = -\rho \text{sign}(\sigma)$$

(a) Predict the parameters of the limit cycle by solving the harmonic balance equation.
(b) Confirm the results via computer simulation.

Exercise 5.2. Repeat Exercise 5.1 assuming that the system is controlled by the twisting controller

$$u = -0.8\text{sign}(\sigma) - 0.6\text{sign}(\dot{\sigma})$$

Exercise 5.3. Repeat Exercise 5.1 assuming that the system is controlled by the super-twisting controller

$$u(t) = u_1(t) + u_2(t)$$

$$\dot{u}_1 = -\gamma \text{ sign}(\sigma)$$

$$u_2 = \begin{cases} -\lambda |s_0|^\rho \text{ sign}(\sigma), & \text{if } |\sigma| > s_0 \\ -\lambda |\sigma|^\rho \text{ sign}(\sigma), & \text{if } |\sigma| \leq s_0 \end{cases}$$

with $\gamma = 0.8$, $\lambda = 0.6$, and $\rho = 0.5$.

Exercise 5.4. Repeat Exercise 5.1 assuming that the system is controlled by the prescribed convergence control law

$$u = -\lambda \text{sign}(\dot{\sigma} + \beta |\sigma|^\rho \text{ sign}(\sigma))$$

where $\lambda = 1$, $\rho = 0.5$ and $\beta = 1$.

Exercise 5.5. Repeat Exercise 5.1 assuming that the system is controlled by the sub-optimal controller

$$u(t) = -U_M \text{sign}(\sigma(t) - \beta \sigma_M(t)) \tag{5.50}$$

with $U_M = 0.1$ and $\beta = 0.2$.

Exercise 5.6. Consider the DC–DC converter presented in Fig. 5.15. The corresponding dynamic equations are given by

$$\begin{array}{rcl} L\frac{di}{dt} & = & -v + u_a V_{in} \\ C\frac{dv}{dt} & = & i - \frac{v}{R} \end{array}$$

where i is the current through the inductor L, v is the voltage across the capacitor C, V_{in} is the input voltage, and $u \in \{0, 1\}$ is the switching control signal. The goal is to stabilize the output voltage v at the desired level v_d.

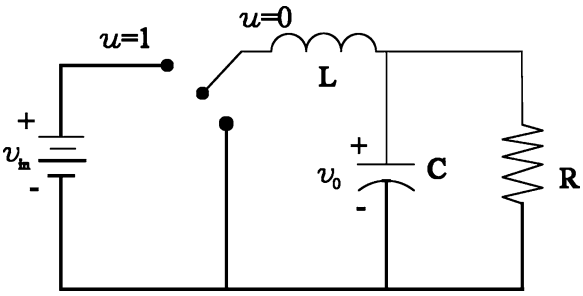

Fig. 5.15 DC–DC Buck converter

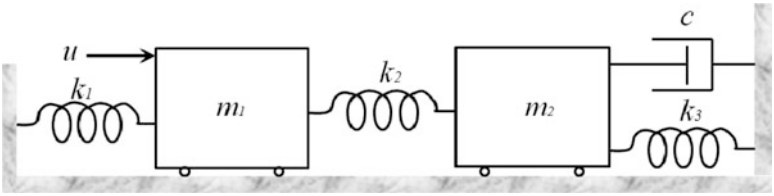

Fig. 5.16 Mass–spring–damper system

Assume that the switching element has the following dynamics:

$$\tau \dot{u_a} = -u_a + u$$

where $u = \frac{1}{2}(1 - \text{sign}(\sigma))$ and $\sigma = v - v_d$.

(a) Predict the parameters of the limit cycle by solving the harmonic balance equation.
(b) Confirm the results via computer simulations.

Exercise 5.7. Consider the mass–spring–damper system presented in Fig. 5.16. The dynamic model of the system is

$$m_1\ddot{x_1} + (k_1 + k_2)x_1 - k_2x_2 = u$$
$$m_2\ddot{x_2} + c\dot{x_2} + (k_3 + k_2)x_2 - k_2x_1 = 0$$

where $m_1 = 1.28$, $m_2 = 1.08$, $k_1 = 190$, $k_2 = 450$, $k_3 = 190$, $c = 15$, and x_1 and x_2 are the positions of the masses m_1 and m_2, respectively. The goal of control is to stabilize the position of m_2 at the origin. Using the suboptimal controller

$$u = -0.1\text{sign}(\sigma - 0.5\sigma_M)$$

where $y = x_2$, compute the parameters of the limit cycle by solving the harmonic balance equation and confirm the results via computer simulation.

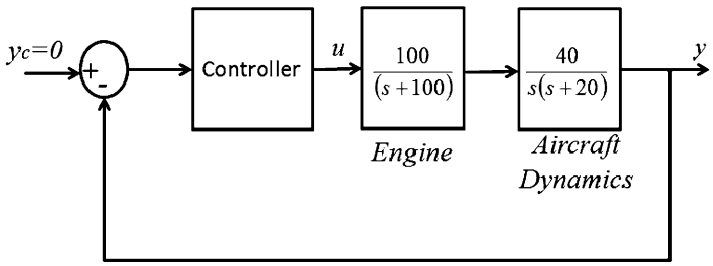

Fig. 5.17 Control system of the heading angle y of the bi-wing aircraft

Exercise 5.8. Consider the disk drive suspension system represented by the transfer functions

$$G_a(s) = \frac{5}{0.001s + 1}; \qquad G_p(s) = \frac{48.78}{s(s + 20)}$$

where $G_a(s)$ is the transfer function of the actuator, named the motor coil, and $G_p(s)$ is the transfer function of the plant, named the arm. Assume the input of the actuator is produced by the twisting algorithm

$$u = -0.8\text{sign}(\sigma) - 0.6\text{sign}(\dot{\sigma})$$

Then compute the parameters of the limit cycle by solving the harmonic balance equation, and confirm the results via a computer simulation.

Exercise 5.9. The heading angle y of a bi-wing aircraft is controlled by the prescribed convergence controller

$$u = -10\text{sign}(\dot{\sigma} + 2|\sigma|^{0.5}\,\text{sign}(\sigma))$$

The block diagram of the control system is given in Fig. 5.17, where the transfer function of the engine is considered as unmodeled dynamics. Compute the parameters of the limit cycle by solving the harmonic balance equation and confirm the results via computer simulation.